Viscosity bounds in liquids with different structure and bonding types

M. Withington [1,*] H. L. Devereux [1] C. Cockrell [2] A. M. Elena [3] I. T. Todorov [3] Z. K. Liu [4]
S. L. Shang [4] J. S. McCloy [5] P. A. Bingham [6] and K. Trachenko [1]

[1]*School of Physical and Chemical Sciences, Queen Mary University of London, Mile End Road, London, E1 4NS, United Kingdom*
[2]*Department of Materials, Imperial College London, Exhibition Road, London, SW7 2AZ, United Kingdom*
[3]*Scientific Computing Department, Science and Technology Facilities Council, Daresbury Laboratory,
Keckwick Lane, Daresbury, WA4 4AD, United Kingdom*
[4]*Department of Materials Science and Engineering, The Pennsylvania State University, University Park, Pennsylvania 16802, USA*
[5]*School of Mechanical and Materials Engineering, Washington State University, Pullman, Washington 99163, USA*
[6]*Materials and Engineering Research Institute, Sheffield Hallam University, Sheffield, S1 1WB, United Kingdom*

Recently, it was realized that liquid viscosity has a lower bound which is nearly constant for all liquids and is governed by fundamental physical constants. This was supported by experimental data in noble and molecular liquids. Here, we perform large-scale molecular dynamics simulations to ascertain this bound in two other important liquid types: the ionic molten salt system LiF and metallic Pb. We find that these ionic and metallic systems similarly have lower viscosity bounds corresponding to the minimum of kinematic viscosity of $\sim 10^{-7}$ m^2/s. We show that this agrees with experimental data in other systems with different structures and bonding types, including noble, molecular, metallic, and covalent liquids. This expands the universality of viscosity bounds into the main system types known.

I. INTRODUCTION

Different liquids are considered for use as coolants in nuclear reactors, including molten salts and metals [1–4]. In these applications, viscosity η and thermal conductivity are two important properties characterising the performance of these liquids and governing their flow/diffusion and thermal transport properties. Understanding and predicting these properties over a range of temperatures and pressures is therefore important from the application point of view. This understanding is also of fundamental theoretical importance, in view that properties of liquids are strongly system dependent and hence are not considered amenable to a general theory, in contrast to solids and gases [5].

Viscosity of low-temperature dense liquids is governed by the activation energy barrier U as

$$\eta = \eta_0 \exp\left(\frac{U}{T}\right), \tag{1}$$

where U is set by the intermolecular interactions and structure in the liquid, T is temperature, and η_0 is the prefactor related to the high-temperature limit of η. Here and below, $k_B = 1$.

Equation (1) applies in the low-temperature liquid-like regime where a molecule oscillates before undergoing a jump into a neighboring quasiequilibrium position [6,7]. In this regime, η increases on cooling and, if crystallization is avoided, can vary by up to 15 orders of magnitude in the viscous regime. At high temperature, the oscillatory component of particle motion is lost. This can occur in either the gas phase at pressures below the critical pressure or above the Frenkel line in the supercritical regime where particle dynamics become purely diffusive [8]. In the gaslike regime of particle dynamics, η follows a different temperature dependence:

$$\eta = \tfrac{1}{3}\rho v L, \tag{2}$$

where ρ is density, v is the average particle speed, L is the particle mean free path, and η increases with temperature as $\eta \propto T^{1/2}$ because $L \propto \frac{1}{\rho}$ and $v \propto T^{1/2}$.

The increase of η at low temperature and its increase at high temperature implies that η has a minimum. It turns out that the value of the minimum of the kinematic viscosity $v = \frac{\eta}{\rho}$, v_m, can be approximately evaluated in terms of fundamental physical constants as [9,10]

$$v_m = \frac{1}{4\pi}\frac{\hbar}{\sqrt{m_e m}}, \tag{3}$$

where m is the mass of the molecule, and m_e is the electron mass.

Deriving Eq. (3) involves two steps. First, it was shown that the minimum of v depends only on two parameters characterizing a condensed matter system: interatomic separation a and the largest Debye vibration frequency ω_D. Second,

characteristic values of a and ω_D are set by the Bohr radius and Rydberg energy. This gives Eq. (3) [9,10].

Equation (3) has explained the longstanding question considered by Purcell and Weisskopf [11], namely, why the viscosity of all liquids never falls below a certain value comparable with the viscosity of water at room conditions. The answer comes in two parts [12]. First, viscosities stop decreasing because they have minima. Second, those minima are largely fixed by fundamental constants in Eq. (3) ($\nu_m \propto \frac{1}{\sqrt{m}}$ does not change ν_m too much for most liquids).

In addition to liquids, viscosity minima have been of interest in other areas of physics, including holographic models based on the correspondence between strongly interacting field and gravity theories [13]. More generally, understanding the origin of bounds on system properties has enthralled physicists, including those interested in collective dynamics and systems where many interacting agents operate. Apart from the interest in the values and origins of the bounds themselves, there is another reason why these bounds are important: finding and understanding bounds on physical properties often means that we enhance our grasp of or clarify the underlying physics of the property in question [10,14,15].

In addition to viscosity, it was realized that Eq. (3) provides a lower bound for an unrelated property of liquids: thermal diffusivity α [16]. As discussed earlier, this property is directly relevant to industrial properties where molten salts are used, including the operation of coolants in nuclear reactors, where the heat transfer processes are important.

The lower bound ν_m in Eq. (3) is of the order of 10^{-7} m^2/s (this value corresponds to m equal to the proton mass which sets the magnitude of atomic masses). This agrees with experimental viscosity minima for noble, molecular, and network liquids to within a factor of 1–3 [9]. It was also found to agree with the experimental high-temperature limiting value of viscosity of metallic alloys [15,17]. This analysis was further extended in Ref. [18].

However, no estimations of viscosity minima in molten salts have been undertaken experimentally due to high melting points and hence very high temperatures required to reach the minima. It therefore remains unknown how the viscosities of molten salts conform to the presumably universal crossover between the liquidlike and gaslike regimes and to the theoretical minimum in Eq. (3). Apart from theoretical importance, knowledge of this would be important from the application point of view: knowing the pressure and temperature conditions of the minima of kinematic viscosity and thermal diffusivity would enable predictions of the optimal state of operation of molten salts.

Here, we perform large-scale molecular dynamics (MD) simulations of the molten salt LiF as a case study (LiF is a common component in molten salt mixtures used in nuclear reactors [2]). We also simulate metallic Pb. We find that these ionic and metallic systems have lower viscosity bounds corresponding to the minimum of kinematic viscosity of $\sim 10^{-7}$ m^2/s. We show that this agrees with the experimental data in other systems with different structures and bonding types, including noble, molecular, metallic, and covalent liquids. This expands the universality of viscosity bounds into the main types of systems known.

II. METHODS

We use the DL_POLY MD package [19]. For LiF, we used the empirical potential as in the previous work [20–22] with parameters derived earlier [23]. For Pb, we used the potential from Ref. [24]. We also simulated liquid Ar using the standard Lennard-Jones potential.

Unless otherwise stated, we simulated for 1 000 000 time steps, with a fixed simulation time step of 0.001 ps. The system size used varied from 2000 atoms in LiF to 5120 in Pb. We have also simulated larger systems with 100 000 particles and found that the values of viscosity collected were consistent regardless of the system size. Similar behavior of measured viscosities with system size has been found previously [25]. We simulated a wide range of temperatures for each pressure. We first equilibrated the system at each pressure in the constant-pressure ensemble for 20 000 steps and then performed production runs for 1 000 000 steps in the constant energy and volume ensemble where the data were collected for calculating properties.

The dynamic viscosity η was calculated using the Green-Kubo method [26,27] as

$$\eta = \frac{V}{T} \int_0^\infty dt \langle P_{xy}(0)P_{xy}(t)\rangle, \tag{4}$$

where V is the volume of the system, and P_{xy} is the xy component of the stress tensor.

Obtaining accurate statistics via the Green-Kubo method is a well-known computational issue [28], which we address by averaging statistics over 20 independent initial conditions. This has been sufficient in prior work involving viscosity calculations [25].

We also calculate the kinematic viscosity $\nu = \frac{\eta}{\rho}$ governing the nonequilibrium flow and other properties such as, for example, fuel atomization quality [29]. Density ρ was calculated at the same state points as η.

III. RESULTS AND DISCUSSION

We show the calculated η in Fig. 1(a) for two different systems sizes. We observe good agreement of η calculated in the two systems. We also observe agreement with the earlier MD results in the low-temperature range using the same potential [22]. Little experimental data for LiF viscosity exists >1000 K. We use the experimental data from Ref. [30], which contains the widest range of data and was found to be in agreement with other experiments in the low-temperature range [31,33]. The MD results underestimate the experimental viscosity by a factor of $\sim$1.3–5; however, the overall shape of η is similar in experimental and MD data. As discussed in Ref. [22], the simulated viscosity is lower than experimental viscosity due to the model not accurately matching the melting point, $\sim$300 K lower than experimental values (predicting melting points accurately is a more general problem in atomistic simulations due to several factors including short simulation times which can be insufficient to exceed slow kinetics of phase transformations). Translating all temperatures upward by this melting point discrepancy of 300 K while maintaining all values of viscosity results in much better agreement, demonstrating that the empirical
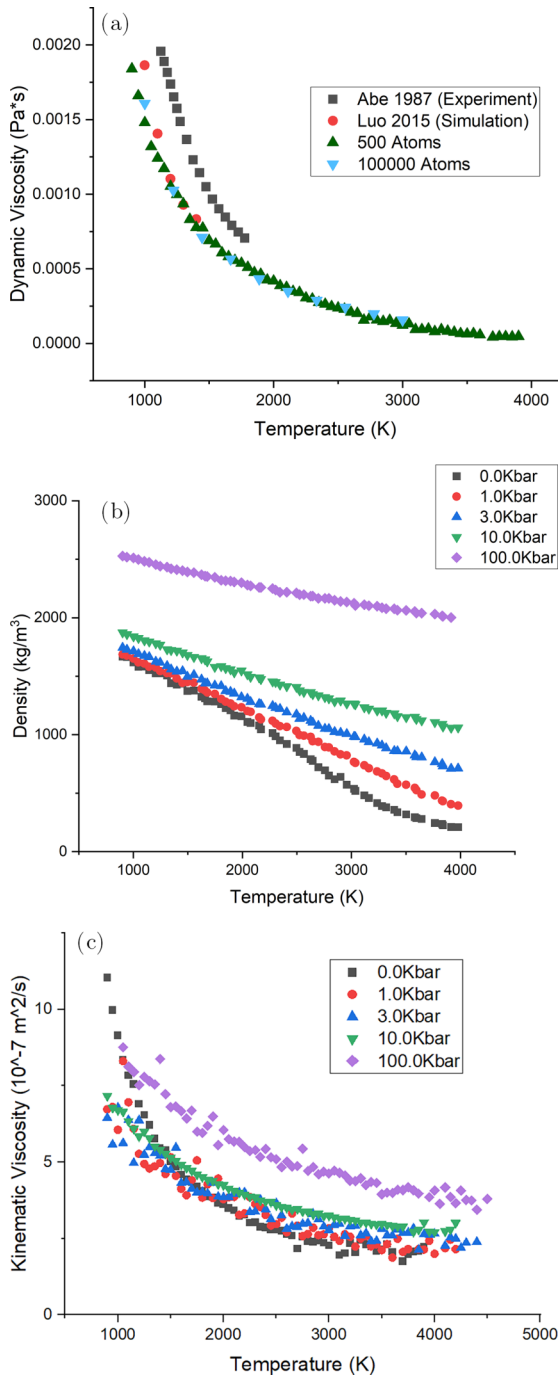
FIG. 1. (a) Dynamic viscosity of LiF for small (500 atoms) and large (100 000 atoms) systems. We compare with earlier molecular dynamics (MD) results [22] as well as experimental results in Ref. [30], which have been shown to have good agreement with more recent experiments [31,32]. (b) Density at different pressures. (c) Kinematic viscosity of LiF simulated using 2000 atoms for a range of pressures.

potential accurately models the dissipative dynamics of the liquid. We note that the underestimation of the melting point does not affect our results since we are interested in the values of viscosity minima.

We observe that the calculated η tends to an approximately constant value of about $\eta = 2 \times 10^{-4}$ Pa s at high

temperature. This is close to viscosity minima in noble, molecular, and network liquids [9]. Simulating higher temperature results in the known instability of the Born-Mayer potential at short distances. This could be fixed by, for example, adding short-range repulsive terms to the potential (e.g., in the form of Ziegler-Biersack-Littmark potentials [34]); however, this is not required for the purposes of this paper, in which we aimed at evaluating the limiting lower viscosity bounds.

Density as a function of temperature is shown in Fig. 1(b) for different pressures. We observe that the slope of density decrease becomes smaller at high pressure, corresponding to the decrease of the thermal expansion coefficient with pressure. This is consistent with the common behavior seen in solids [35].

The calculated kinematic viscosity $\nu = \frac{\eta}{\rho}$ is shown in Fig. 1(c) for different pressures. We make several observations. First, ν reaches a constant value at high temperature and shallow minima at low pressures. The minima become more apparent here, compared with in the dynamic viscosity in Fig. 1(a), due to the decrease of density at high temperature. Second, pressure increases the values of the minima and constant values at which ν tends to a constant at high temperature. This is like what is observed in noble, molecular, and network liquids [9] and is related to the increase of the activation energy for molecular rearrangement with pressure and associated increase of viscosity. Third, the value of ν at their constant value or minima is in the range 2×10^{-7} to $5 \times 10^{-7} \mathrm{m^2/s}$. This is of the same order, $10^{-7} \mathrm{m^2/s}$, as predicted by Eq. (3). This last point is important and implies that the viscosities of ionic systems and molten salts have the same behavior in terms of the value of their viscosity minima. We will make the comparison between calculated and theoretical values more quantitative later on, alongside the other liquids we study.

Here, η and ν for the simulated metallic system Pb are shown in Fig. 2. These show very similar results to those of LiF. Here, η increases with pressure and tends to about $\eta = 2 \times 10^{-4}$ Pa s at high temperature. Also, ν has a minimum $\sim 2 \times 10^{-7} \mathrm{m^2/s}$ at low pressure, as predicted by Eq. (3). To emphasize this similarity, we plot ν for Pb, LiF, and Ar in Fig. 2(c).

To compare our results for ionic LiF and metallic Pb with a wider dataset, we add the experimental η and ν for noble Ar and molecular CH_4 and CO_2 as well as network H_2O [36] to the plots in Fig. 3. It is appropriate to note here that, differently from noble and molecular liquids, the NIST database [36] does not include viscosities of ionic molten salts and metallic systems. Part of the issue is the experimental difficulty related to high melting and boiling points of these systems. The value of our current simulations therefore includes provision of these data and serves as a guide for future high-temperature experiments.

The results collected in Fig. 3 are consistent with what is expected for the dependence of viscosity on temperature, as discussed in the introduction: the decrease with temperature in the liquidlike regime, followed by its increase in the gaslike regime. We observe a great amount of variation in the values of viscosity collected for different systems as well as the variability of the shape of viscosity curves. We also observe
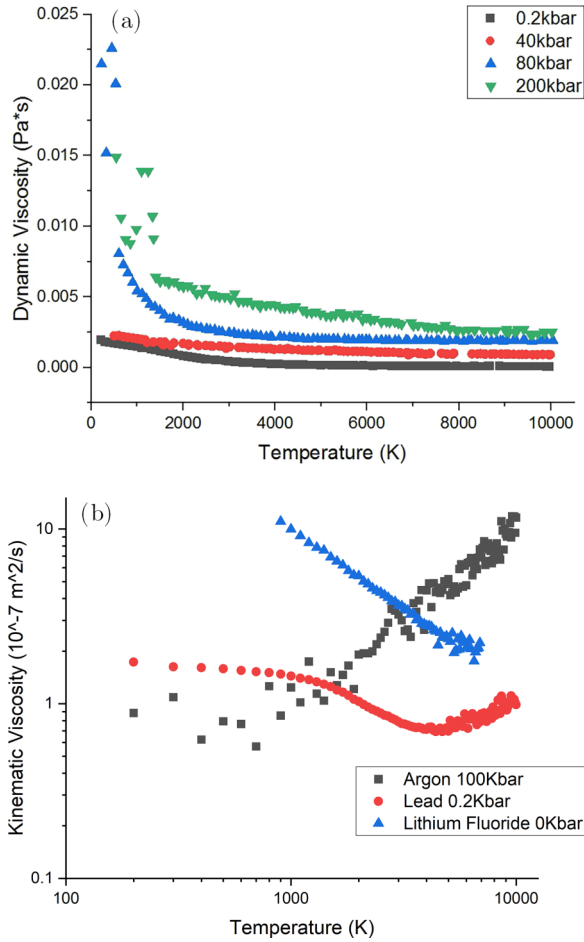
FIG. 2. (a) Dynamic viscosity of Pb at 0.2, 40, 80, and 200 kbar. (b) Comparison of kinematic viscosity of Ar, Pb, and LiF.
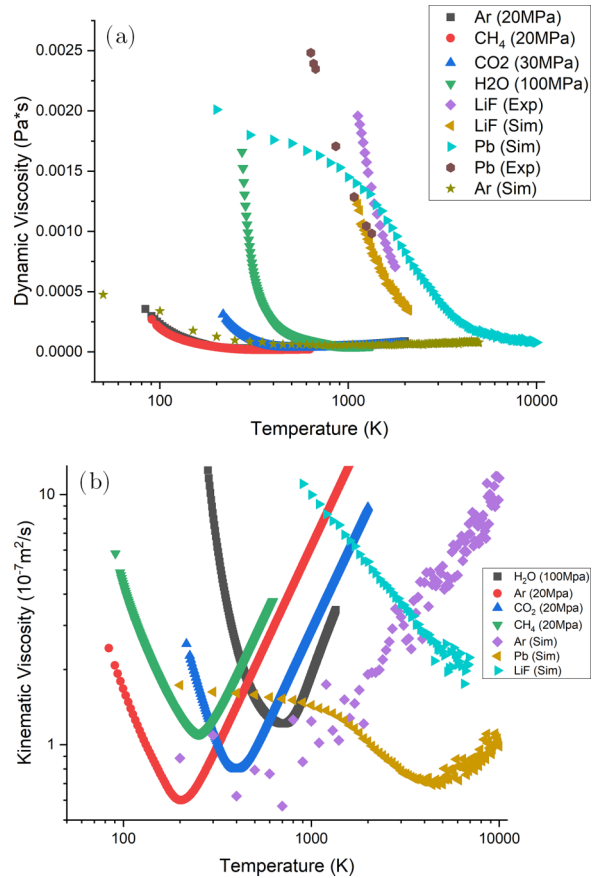

FIG. 3. (a) Experimental and simulated dynamic viscosity for LiF, Pb, and Ar. In order: NIST dataset for Ar 20 MPa, CH_4 20 MPa, CO_2 30 MPa, H_2O 100 MPa [36], LiF experiment [30], our LiF simulation, our Pb simulation, Pb experiment [37], and our Ar simulation. (b) Kinematic viscosity of systems in (a).

a consistency in the magnitude of the minimum values of viscosity, in agreement with Eq. (3) predicting close values of the lower viscosity bound in all liquids. This includes the ionic molten salt LiF and metallic Pb.

We now address the quantitative comparison between the predicted and calculated ν_m. In Table I, we show theoretical and calculated ν_m for LiF, Pb, and Ar. The ratio between calculated and theoretical values is in the range 1.7–4.6. This is like the range of ratios for the large set of noble, molecular, and network liquids found earlier, where this ratio is in the range 0.5–3 [9].

TABLE I. Comparison of predicted values calculated from the formula against simulated or experimental values of the kinematic viscosity minimum, $\nu_m 10^{-8}$ m²/s.

Liquid	Theory	Simulated	Experimental
LiF	6.0	18.8	
Pb	1.5	6.9	
Ar (20 MPa)	3.4	5.7	5.9
CH_4 (20 MPa)	5.4		11.0
CO_2 (30 MPa)	3.2		8.0
H_2O (100 MPa)	5.1		12.1

The difference between theoretical and observed ν_m by a factor of 1–4 is related to a number of approximations involved in deriving Eq. (3). This includes approximating the interatomic separation by the Bohr radius and the bonding energy by the Rydberg energy. Recall that the main purpose of Eq. (3) is twofold: first, it shows that the viscosity minimum is largely the same for all liquids because it is set by fundamental physical constants. Second, Eq. (3) serves to evaluate a characteristic value, order of magnitude, of ν_m.

We have discussed viscosity minima in ionic, metallic, noble, molecular, and network liquids. This leaves the remaining important bonding type: covalent. Silica is a commonly discussed system in which covalency is strong: It is a system with mixed bonding where covalency and ionicity make similar contributions to the bonding type. Experimentally, viscosity of silica was measured up to ~3000 K, and yet no minimum was seen due to challenges involved in high-temperature experiments [38]. Simulated silica, taken to yet higher temperature in excess of 6000 K, shows saturation to a constant value of ~10^{-3} Pa s [39]. This corresponds to ν_m of ~5 × 10^{-7} m²/s and falls in the range of ν_m predicted theoretically by Eq. (3).

An interesting observation from Eq. (3) is that the minimal viscosity is a quantum property and approaches zero in the

classical limit $\hbar = 0$. This might be perceived to be at odds with our thinking about liquids as mostly high-temperature classical systems. However, the nature and origin of interatomic forces and radii are quantum mechanical, and Eq. (3) reminds us of this [12]. This then brings the question of how our classical MD simulations reproduce the lower bound of liquid viscosity, the essentially quantum effect. We understand this if we recall that the parameters of empirical potentials in classical MD simulations are tuned to result in interatomic separations and energy values in real systems (either by fitting to experiments or quantum-mechanical simulations) where they are quantum mechanical in origin. The classical simulations capture quantum effects, including the lower viscosity bound, through these potential parameters.

IV. SUMMARY

We have explored the nature of viscosity minima in ionic molten salt liquid LiF, complemented by metallic Pb. We have found that these systems have lower viscosity bounds corresponding to the minimum of kinematic viscosity of $\sim 10^{-7}$ m^2/s. This agrees with the experimental data for other systems with different structures and bonding type, including noble, molecular, metallic, and covalent liquids, and it

expands the universality of viscosity bounds into the main types of systems known. In future work, it may be interesting to develop more accurate potentials or employ quantum-mechanical MD simulations to simulate molten salts.

We have previously found that Eq. (3) also gives the minima of an unrelated yet important property: thermal diffusivity [16]. This was supported by the experimental data for noble and molecular systems. Our current findings therefore suggest that, like the kinematic viscosity, the minima of thermal diffusivity are more universal and include other system types including the ionic molten salts. This would be interesting to explore in future work.

[1] M. W. Rosenthal, P. R. Kasten, and R. B. Briggs, Nucl. Appl. Technol. **8**, 107 (1970).

[2] B. A. Frandsen, S. D. Nickerson, A. D. Clark, A. Solano, R. Baral, J. Williams, J. Neuefeind, and M. Memmott, J. Nucl. Mater. **537**, 152219 (2020).

[3] T. Allen and D. Crawford, Sci. Technol. Nucl. Install. **2007**, 097486 (2007).

[4] L. Tang, J. Xiong, W. Wan, Z. Guo, W. Zhou, S. Huang, and H. Zhong, Ceram. Int. **41**, 3420 (2015).

[5] L. D. Landau and E. M. Lifshitz, *Course of Theoretical Physics, Statistical Physics, Part 1* (Pergamon Press, Oxford, 1970), Vol. 5.

[6] J. Frenkel, *Kinetic Theory of Liquids* (Oxford University Press, Oxford, 1947).

[7] J. C. Dyre, Rev. Mod. Phys. **78**, 953 (2006).

[8] C. Cockrell, V. V. Brazhkin, and K. Trachenko, Phys. Rep. **941**, 1 (2021).

[9] K. Trachenko and V. V. Brazhkin, Sci. Adv. **6**, eaba3747 (2020).

[10] K. Trachenko, Adv. Phys. **70**, 469 (2021).

[11] E. M. Purcell, Am. J. Phys. **45**, 3 (1977).

[12] K. Trachenko and V. V. Brazhkin, Phys. Today **74**(12), 66 (2021).

[13] P. K. Kovtun, D. T. Son, and A. O. Starinets, Phys. Rev. Lett. **94**, 111601 (2005).

[14] S. Grozdanov, Phys. Rev. Lett. **126**, 051601 (2021).

[15] A. K. Gangopadhyay, Z. Nussinov, and K. F. Kelton, Phys. Rev. E **106**, 054150 (2022).

[16] K. Trachenko, M. Baggioli, K. Behnia, and V. V. Brazhkin, Phys. Rev. B **103**, 014311 (2021).

[17] J. Xue, F. S. Nogueira, K. F. Kelton, and Z. Nussinov, Phys. Rev. Res. **4**, 043047 (2022).

[18] S. A. Khrapak and A. G. Khrapak, Phys. Fluids **34**, 027102 (2022).

[19] I. T. Todorov, W. Smith, K. Trachenko, and M. T. Dove, J. Mater. Chem. **16**, 1911 (2006).

[20] M. C. C. Ribeiro, J. Phys. Chem. B **107**, 4392 (2003).

[21] V. Sarou-Kanian, A.-L. Rollet, M. Salanne, C. Simon, C. Bessada, and P. A. Madden, Phys. Chem. Chem. Phys. **11**, 11501 (2009).

[22] H. Luo, S. Xiao, S. Wang, P. Huai, H. Deng, and W. Hu, Comput. Mater. Sci. **111**, 203 (2016).

[23] M. Sangster and M. Dixon, Adv. Phys. **25**, 247 (1976).

[24] D. Belashchenko, Russ. J. Phys. Chem. A **86**, 779 (2012).

[25] C. Cockrell, V. V. Brazhkin, and K. Trachenko, Phys. Rev. E **104**, 034108 (2021).

[26] U. Balucani and M. Zoppi, *Dynamics of the Liquid State* (Oxford University Press, Oxford, 1994).

[27] R. Zwanzig and R. D. Mountain, J. Chem. Phys. **43**, 4464 (1965).

[28] Y. Zhang, A. Otani, and E. J. Maginn, J. Chem. Theory Comput. **11**, 3537 (2015).

[29] M. Das, in *Encyclopedia of Renewable and Sustainable Materials*, edited by S. Hashmi and I. A. Choudhury (Elsevier, Oxford, 2020), pp. 202–211.

[30] Y. Abe, O. Kosugiyama, and A. Nagashima, J. Nucl. Mater. **99**, 173 (1981).

[31] T. Ejima, Y. Sato, S. Yaegashi, T. Kijima, E. Takeuchi, and K. Tamai, J. Jpn. Inst. Met. **51**, 328 (1987).

[32] A.-M. Popescu and V. Constantin, Chem. Eng. Commun. **202**, 1703 (2015).

[33] C. Merlet, P. A. Madden, and M. Salanne, Phys. Chem. Chem. Phys. **12**, 14109 (2010).

[34] J. F. Ziegler, J. P. Biersack, and U. Littmark, *The Stopping and Range of Ions in Matter* (Pergamon Press, New York, 1985).

[35] O. L. Anderson, *Equations of State of Solids for Geophysical and Ceramic Science* (Oxford University Press, Oxford, 1995).

[36] National Institute of Standards and Technology Database, https://webbook.nist.gov/chemistry/fluid (2023).

[37] D. Ofte, J. Nucl. Mater. **22**, 28 (1967).

[38] M. I. Ojovan and W. E. Lee, J. Appl. Phys. **95**, 3803 (2004).

[39] J. Horbach and W. Kob, Phys. Rev. B **60**, 3169 (1999).

[40] T. King, S. Butcher, and L. Zalewski, Apocrita—High Performance Computing Cluster for Queen Mary University of London (Queen Mary University of London Technical Report, 2017).